

Coherent Propagation of X Rays in a Planar Waveguide with a Tunable Air Gap

M. J. Zwanenburg,¹ J. F. Peters,¹ J. H. H. Bongaerts,¹ S. A. de Vries,² D. L. Abernathy,³ and J. F. van der Veen¹

¹*Van der Waals-Zeeman Institute, University of Amsterdam, Valckenierstraat 65, 1018 XE, Amsterdam, The Netherlands*

²*FOM Institute for Atomic and Molecular Physics, Kruislaan 407, 1098 SJ, Amsterdam, The Netherlands*

³*European Synchrotron Radiation Facility, B.P. 220, 38043 Grenoble Cedex, France*

(Received 20 October 1998)

We have made a multimode waveguide of x rays having an air gap as the guiding medium. Individual transverse electric modes were found to propagate through the planar waveguide with essentially no attenuation and with negligible scattering losses to other modes. If different modes are excited simultaneously at the waveguide entrance, then the phase relation between these modes as given by their propagation constants is found to be preserved over the entire length of the waveguide. [S0031-9007(99)08517-8]

PACS numbers: 61.10.-i, 07.85.Qe, 41.50.+h

For more than 20 years thin-film structures have been used as waveguides for x rays [1]. These planar waveguides have in common with their optical counterparts that there is a thin central layer having a higher refractive index than the surrounding media. As a result of total internal reflections from the interfaces, the layer is capable of guiding a finite number of electromagnetic (e.m.) modes which propagate in the plane of the layer and have a standing-wave character in the direction normal to the plane. The modes are evanescent in the surrounding media. For x rays, the refractive index of a medium is slightly less than one, i.e., $n = 1 - \delta - i\beta$, where $\delta \sim 10^{-6}$ and $\beta \sim 10^{-8}$ are proportional to the electron density and the absorption coefficient, respectively. Hence, the guiding layer material should be less dense than the surrounding material.

We have constructed a planar x-ray waveguide consisting of two parallel plates of a few mm in length, which can be accurately positioned at a distance of a few hundred nanometers. Waveguiding takes place in the narrow air gap between the plates. In previous devices the guiding layer was a deposited layer of a light element such as carbon [2,3]. At 0.1 nm wavelength, a substantial fraction of the x-ray beam is absorbed in these materials. By comparison, the absorption in air is negligible. Low-loss transport of x rays has earlier been achieved in hollow glass capillaries [4], which in tapered form are primarily used as focusing devices. However, coherent excitation of discrete modes is not possible in a tapered geometry. In this Letter we report for the first time the excitation and propagation of single coherent x-ray modes in a waveguide with an air gap. Apart from being a loss-free transport medium, the waveguide may serve as a sample (e.g., liquid) container enabling coherent x-ray scattering experiments on samples of nanometer thickness in a wave field with accurately known amplitude and phase at each point. In a first, essential, step towards achieving this goal we demonstrate the waveguiding properties of a planar geometry in the absence of a sample. The undisturbed propagation of single modes at

x-ray wavelengths requires nanometer control of the plate distance and parallelism and requires the plates to be flat and atomically smooth.

The incident field is determined by the geometry of our experiment as shown in Fig. 1. Let z and x be the coordinates along the propagation direction and along the normal to the plates, respectively. A plane e.m. wave, with wave number k and with the electric field polarized perpendicular to the plane of incidence, is incident onto the device at a grazing angle. In front of the waveguide entrance the wave is totally reflected from the large bottom plate. The resulting field across the entrance plane ($z = 0$) is a standing wave due to interference of the incident wave and the reflected wave. The standing wave field must have a node at the surface of the bottom plate ($x = 0$) and is of the form $\Psi(x, z = 0) = \sin(k\theta_i x)$, where θ_i is the angle of incidence. For a gap of width W this field will also have a node at the position of the upper plate if $\theta_i = \theta_m$, with $\theta_m = (m + 1)\pi/kW$ and $m = 0, 1, 2, \dots$. This wave field, which excites the m th transverse-electric (TE) mode of the waveguide, will propagate through the waveguide undisturbed. The corresponding expression for the amplitude of the wave field within the waveguide is to a good approximation given by

$$\Psi_m(x, z) = \sin(k\theta_m x) \exp(-i\beta_m z), \quad (1)$$

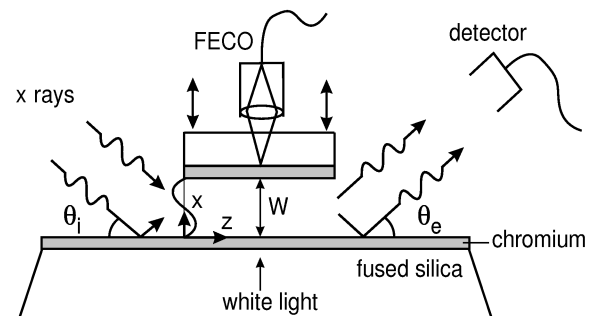


FIG. 1. Schematic of the waveguide and the experimental geometry. Angles and distances are not to scale; see text.

where $\beta_m = k\sqrt{(1 - \theta_m^2)} \approx k(1 - \theta_m^2/2)$ is the propagation constant of the mode [5]. Within the plate material, the field decays exponentially to zero. The $1/e$ decay depth for the m th mode equals $\xi = k^{-1}(\theta_c^2 - \theta_m^2)^{-1/2}$ with θ_c the critical angle for total internal reflection [5]. For the lower mode numbers and the experimental conditions considered here, we have $\xi \ll W$. Hence, the contribution of the evanescent field to the propagation of these modes is negligible, which justifies the assumption in (1) that $\Psi_m(0, z) = \Psi_m(W, z) = 0$.

For angles of incidence $\theta_i \neq \theta_m$, the wave field amplitude at the entrance plane is not zero at $x = W$, and therefore a coherent superposition of guided modes is needed to match the incident field. The corresponding wave field is given by the Fourier expansion

$$\Psi(x, z) = \sum_{m=0}^{m_{\max}} c_m(\theta_i) \Psi_m(x, z), \quad (2)$$

with

$$c_m(\theta_i) = \frac{2(-1)^m}{kW} \frac{\theta_m \sin(k\theta_i W)}{(\theta_m^2 - \theta_i^2)}. \quad (3)$$

Here, $\Psi_m(x, z)$ is given by (1) and $m_{\max} \approx kW\theta_c/\pi - 1$ is the maximum mode number allowed up to the critical angle θ_c . Modes with number m larger than m_{\max} cannot be confined within the gap and will be absorbed by the plate material ("radiative" modes [5]). For an incident angle θ_i in between two consecutive guided-mode angles θ_m , the amplitude is distributed predominantly over the two neighboring modes.

The waveguide was made of two fused-silica plates with an optical flatness of $< \lambda/20$, coated with a thin metal film. Chromium layers of 30 nm thickness were sputter-deposited onto the bottom plate (o.d. = 25 mm) and thermally evaporated onto the upper plate (o.d. = 5.2 mm). The surfaces had an rms roughness of 0.3 and 0.4 nm, respectively. These values were determined from x-ray reflectivity measurements on each of the plates. The upper plate was mounted onto a piezo element which in turn was mounted onto a tripod of piezodriven Inchworm[®] motors. The Inchworms were used for a coarse approach to the lower plate and for angular adjustments. The additional piezo element was used for fine tuning the gap. The gap width W can be varied down to 250 nm while keeping the plates parallel. In order to compensate for thermal drifts we continuously monitored and adjusted the plate distance to within an accuracy of 2 nm by using the optically semitransparent plates as an interferometer based on the technique of fringes of equal chromatic order (FECO) [6]. The latter technique also enables us to eliminate a possible tilt angle between the plates to within an accuracy of 5 μ rad. Note that a gap distance of 250 nm over a length of 5.2 mm results in a length-to-width ratio as large as 2×10^4 .

The waveguide setup was mounted horizontally onto the diffractometer at the undulator beam line ID10A

(Troika) of the European Synchrotron Radiation Facility (ESRF) in Grenoble (France) [7]. A photon energy of 16.5 keV ($\lambda = 0.0751$ nm) was selected using the (111) reflection of a diamond crystal monochromator in Laue geometry followed by a mirror for suppression of higher harmonics from the undulator. The intensity of the beam of 0.1 mm width passing through a vertical gap of 500 nm was typically 2.4×10^7 photons/s. The transverse coherence length L_v of the beam in the vertical plane along the coordinate x is determined by $L_v = \lambda D/\sigma_v = 144 \mu$ m, where $D \approx 45$ m is the distance from the source to the sample and $\sigma_v = 23.5 \mu$ m the vertical source size (full width at half maximum) of the beam. The incident field is fully coherent across the gap since L_v is much larger than the typical gap sizes used in the experiment. In the horizontal plane the source size equals 928 μ m, which yields a transverse coherence length $L_h = 3.6 \mu$ m. As L_h is much smaller than the horizontal beam width of 0.1 mm, the beam has incoherent properties in this direction. The longitudinal coherence length equals $L_l = \lambda^2/\Delta\lambda = 1.5 \mu$ m, with $\Delta\lambda/\lambda = 5 \times 10^{-5}$ the monochromator bandwidth [7]. L_l is to be compared with the maximum path length difference $\text{PLD}_{\max} \approx L(\theta_c^2 - \theta_0^2)/2$ between the highest and lowest modes after traveling over the length of the waveguide. For $L = 5.2$ mm we find $\text{PLD}_{\max} \approx 26$ nm and we conclude that $L_l \gg \text{PLD}_{\max}$. Hence, the nonzero bandwidth of the monochromator does not affect the coherent phase relation between different guided modes.

Given an angular spacing $\Delta\theta_m = \pi/kW$ between modes of typically 0.005° and a vertical beam divergence being much smaller than this value, it is possible to excite only one mode at a time. The total number of guided modes m_{\max} is determined by the critical angle for total reflection from the chromium layer which equals $\theta_c = 0.18^\circ$. For a gap width of 400 nm we find $m_{\max} = 33$.

The modes propagating through the waveguide for a given incidence angle θ_i are identified by measurement of the far-field angular distribution of intensity exiting the waveguide. The diffracted intensity was recorded as a function of the exit angle θ_e by a NaI scintillating detector which can be rotated in the vertical plane. A slit in front of the detector fixes the vertical opening angle at 0.0005° . The presence of the reflecting bottom plate behind the exit plane causes interference between the direct and specularly reflected waves emerging from the exit, making it the time-reversed case of the interference occurring at the front of the waveguide. We measured the diffraction patterns for a range of fixed incidence angles θ_i up to a value corresponding to excitation of the 11th TE mode. Figure 2 shows a logarithmic contour plot of the intensity over a mesh of angle pairs (θ_i, θ_e) , in steps of $\Delta\theta_i = 0.001^\circ$ and $\Delta\theta_e = 0.0005^\circ$. The peaks along the diagonal at mode angles $\theta_i = \theta_m$, are the unperturbed guided modes. Their angular spacing

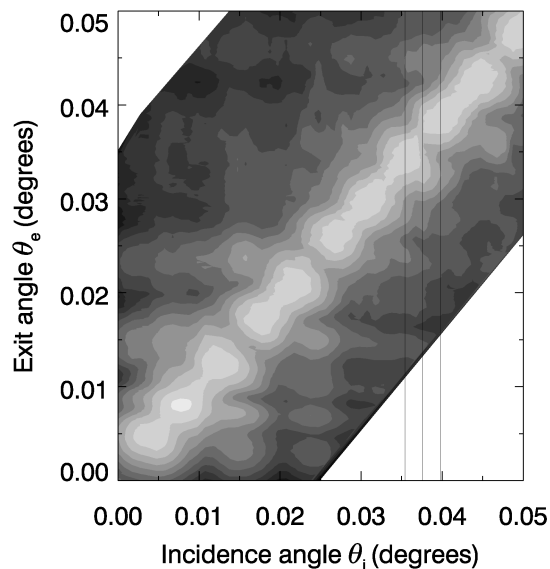


FIG. 2. Logarithmic contour plot of the intensity diffracted from the exit of the waveguide as a function of θ_i and θ_e . The measurements were performed at a wavelength $\lambda = 0.0751$ nm and for $W = 486$ nm and $L = 5.2$ mm. The TE modes in the waveguide are the maxima along the diagonal $\theta_e = \theta_i$.

($\Delta\theta_m \approx 0.0044^\circ$) corresponds to a gap width W of 486 nm, which confirms the interferometrically measured gap width. The off-diagonal peaks at the mode angles are subsidiary diffraction maxima associated with the finite width of the gap. For θ_i in between mode angles θ_m and θ_{m+1} , the field amplitude within the waveguide is distributed over a complete set of modes, but mainly the neighboring ones. Figure 3 illustrates this for patterns along the vertical lines in Fig. 2, which were taken at θ_i values equal to θ_7 , $(\theta_7 + \theta_8)/2$, and θ_8 . The corresponding amplitude distributions within the entrance plane are shown as well.

The measured diffraction patterns are compared with the predictions of a mode propagation model based on the wave field amplitude as given by (2). Applying the Huygens principle to the wave fronts departing from the exit plane and including the postreflection one obtains for the diffracted intensity in the far-field limit

$$I(\theta_i, \theta_e) = \left| \sum_{m=0}^{m_{\max}} e^{-i\beta_m L} c_m(\theta_i) c_m(\theta_e) \right|^2, \quad (4)$$

where I has been normalized such that $I(\theta_m, \theta_m) = 1$. The calculated positions and heights of the diffraction minima are in good agreement with the measurements (dashed curves in Fig. 3). However, the observed phase contrast is smaller than calculated. This probably relates to a partial incoherence of the beam in the vertical plane, which is caused by the optical elements along the incident beam path [8]. We find a better fit to the measured diffraction patterns if $I(\theta_i, \theta_e)$ as given by (4) is convoluted with a Gaussian distribution in θ_i having a full width at half maximum of 0.0033° (solid curves in

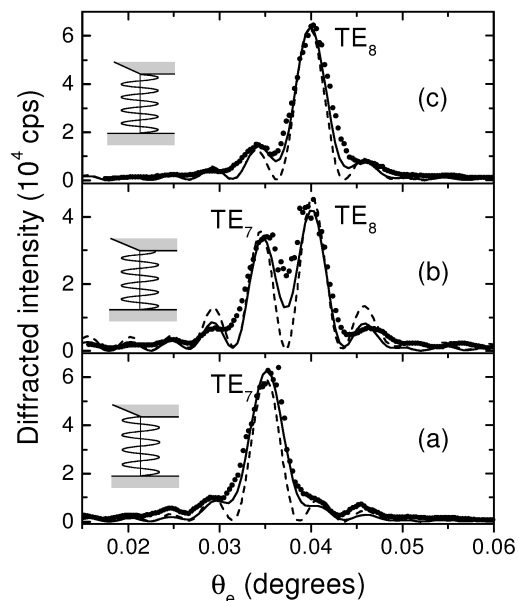


FIG. 3. Diffraction patterns from the exit of the waveguide for different angles of incidence θ_i corresponding with the vertical lines in Fig. 2. The values of θ_i are (a) θ_7 , (b) $(\theta_7 + \theta_8)/2$, and (c) θ_8 . The dashed curves are patterns calculated with the use of (4). The solid curves have been obtained by convoluting $I(\theta_i, \theta_e)$ in (4) with a Gaussian intensity distribution in θ_i ; see text.

Fig. 3). It is as yet unclear which optical elements are responsible for the reduced phase contrast.

Deviations between measurements and calculations are found at higher subsidiary maxima of the diffraction pattern for $\theta_i = (\theta_7 + \theta_8)/2$ [Fig. 3(b)]. This part of the spectrum is sensitive to the change of the field amplitude at $x = W$, where it has to drop sharply to zero. Given the good fits, there is no indication that modes are excited by surface imperfections, as was previously found in solid waveguiding structures [9].

The transmission of the waveguide was determined by opening the detector so as to capture all of the intensity emerging from the exit and recording the intensity as a function of θ_i (not shown). It was verified that this measurement gives the same results as integrating over vertical lines in the contour plot. For θ_i values midway between the lower mode angles (e.g., between modes 1 and 2) the transmission was found to be typically 98.5%. The 1.5% loss is due to scattering into radiative modes and its magnitude is consistent with $\sum_{m=m_{\max}}^{\infty} c_m^2(\theta_i) \approx 0.012$ at these angles.

The specular reflectivity of the waveguide, i.e., the diffracted intensity at $\theta \equiv \theta_e = \theta_i$, has its maximum value at each mode angle θ_m . At other angles the reflectivity is smaller because of destructive interference between modes; see the intensity along the diagonal of the contour plot in Fig. 2. Angle-dependent reflectivity curves are shown in Fig. 4 for three different values of W . For the mode spacing, the relation $\Delta\theta_m = \pi/kW$ is once again confirmed. Also a longer-period variation

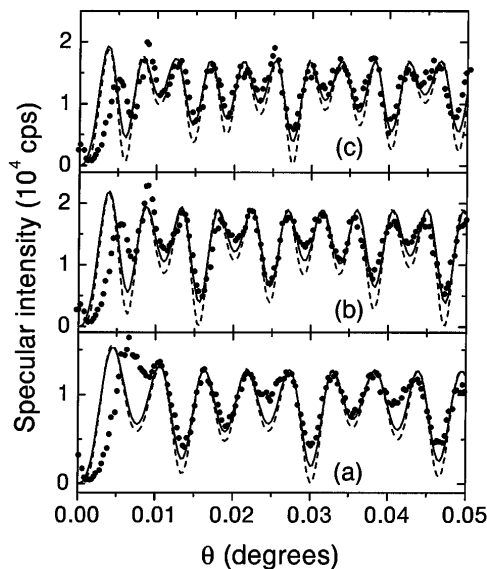


FIG. 4. Diffracted intensities measured along the diagonal $\theta = \theta_e = \theta_i$ in Fig. 2, for gap widths W of (a) 391 nm, (b) 478 nm, and (c) 506 nm. The dashed curves are intensities calculated with the use of (4). The solid curves have been obtained by convoluting (4) with a Gaussian intensity distribution in θ_i ; see text.

of the reflectivity is present, which is due to multimode interference. We have calculated the reflectivity using (4); see dashed curves. The function $I(\theta, \theta)$ multiplied by a constant scaling factor, reproduces the measured reflectivity curves very well, except at the lowest angles where surface irregularities at the entrance may have affected the measurements.

Again, the observed interferences are weaker than calculated and the convolution as described above provides a better fit (solid curves, Figs. 3 and 4). Our observation that the slow periodic variations in the specular reflectivity are in good agreement with the multimode propagation theory [10], is direct proof that the coherence is preserved over the entire length of the waveguide. The latter is quite remarkable. While the number of oscillations made by the e.m. field of a single mode over the distance L is of the order $\beta_m L / 2\pi \sim 10^8$, the difference

$(\beta_m - \beta_n)L / 2\pi \sim 1$ in the number of oscillations between (not too distant) modes m and n is found to remain well defined.

The waveguide is designed to serve as a container of complex fluids such as colloidal suspensions. Inhomogeneities in the refractive index of the fluid cause the amplitude in a single mode to scatter into other modes. Studies of mode coupling enable us to detect layering of the colloidal particles between the confining walls. Ultimately, we would like to reduce the gap width to a few nanometers and study the structural ordering of liquids on a molecular scale in correlation with changes in their lubricating properties.

We would like to thank W. Jark, S. Di Fonzo, and G. Soullie from the Synchrotrone Trieste for their help with the sputter deposition and M. Branicki for his support during the experiments. Discussions with M.K. Smit of Delft University of Technology are gratefully acknowledged. This work was part of the research program of the Foundation for Fundamental Research on Matter (FOM) and was made possible by financial support from the Netherlands Organization for Scientific Research (NWO).

-
- [1] E. Spiller and A. Segmüller, *Appl. Phys. Lett.* **24**, 60 (1974).
 - [2] Y. P. Feng *et al.*, *Phys. Rev. Lett.* **71**, 537 (1993).
 - [3] W. Jark *et al.*, *J. Appl. Phys.* **79**, 4471 (1996).
 - [4] P. Engström, S. Larsson, and A. Rindby, *Nucl. Instrum. Methods Phys. Res., Sect. A* **302**, 546 (1991).
 - [5] D. Marcuse, *Theory of Dielectric Waveguides* (Academic Press, San Diego, 1991).
 - [6] S. Tolansky, *Multiple Beam Interferometry of Surfaces and Films* (Clarendon Press, Oxford, 1949).
 - [7] G. Grübel, J. Als-Nielsen, and A. K. Freund, *J. Phys. IV (France)* **4**, C9-27 (1994).
 - [8] D. L. Abernathy *et al.*, *J. Synchrotron Radiat.* **5**, 37 (1998).
 - [9] Y. P. Feng, H. W. Deckman, and S. K. Sinha, *Appl. Phys. Lett.* **64**, 930 (1994).
 - [10] L. B. Soldano *et al.*, *J. Lightwave Technol.* **13**, 615 (1995).